

POTENTIAL OF THE GLOBAL PRECIPITATION MEASUREMENT CONSTELLATION FOR CHARACTERIZING THE POLAR FIRN

Rahul Kar^{1*}, Mustafa Aksoy¹, Jerusha Ashlin Devadason¹ and Pranjal Atrey²

¹Department of Electrical and Computer Engineering, University at Albany – State University of New York, Albany, NY 12222, USA

²Department of Computer Science, University at Albany – State University of New York, Albany, NY 12222, USA

ABSTRACT

This paper discusses the utilization of the Global Precipitation Measurement (GPM) constellation as a single multi-frequency radiometer to profile subsurface properties of the polar firn. Initial analyses focusing on the Concordia station in Antarctica have demonstrated that GPM brightness temperature measurements can be successfully simulated across a wide frequency spectrum below 100 GHz and are sensitive to important physical properties of the firn from its surface down to deep isothermal ice. Therefore, the GPM constellation provides an excellent opportunity for characterizing the polar firn with broad spatiotemporal coverage.

Index Terms— global precipitation measurement, GPM, microwave radiometry, remote sensing, polar firn, cryosphere

1. INTRODUCTION

Considering the impact of climate change on the Cryosphere, it is important to understand the physics and dynamics of polar ice sheets, and predict future changes in their volume and masses. This is also critical to follow the weather, climate, and water cycle on the Earth [1-2]. The firn temperature, density, and grain size are important indicators for the polar ice mass balance and climate [3-7]. Thus, wide-scale measurements of these parameters are desired. Because of the extreme environmental conditions associated with the polar regions, airborne and spaceborne passive microwave remote sensing are the most suitable techniques for such measurements. Furthermore, electromagnetic penetration depth changes with frequency in ice; thus, wideband or multi-frequency radiometers can profile critical thermal and physical properties of the polar firn versus depth [8]. This paper evaluates the potential of utilizing the Global Precipitation Measurement (GPM) satellite constellation as a multi-frequency (11 frequency channels at 6.9 GHz, 7.3 GHz, 10.65 GHz, 18.7 GHz, 19.35 GHz, 22.235 GHz, 23.8 GHz, 36.5 GHz, 37 GHz, 89 GHz, and 91.665 GHz) microwave

radiometer system to characterize the polar firn through analytical radiation simulations. Sections 2 and 3 summarize the models used in this study for the firn properties and microwave radiation, section 4 describes the GPM instruments relevant to this study, and section 5 discusses the radiation simulation results. Finally, section 6 presents the concluding remarks.

2. POLAR FIRN PROPERTIES

2.1. Firn Density

The vertical density profiles of the polar firn $\rho(z)$ is expressed as the sum of an average firn density and random fluctuations due to internal layerings [9]:

$$\rho(z) = \rho_{\infty} - (\rho_{\infty} - \rho_0)e^{z\beta} + \rho_n(z)e^{z\alpha} \text{ kg/m}^3 \quad (1)$$

where ρ_0 is the near surface density, ρ_{∞} is the compacted ice density at depth, $z < 0$ is depth, and β is a factor that controls the saturation rate of the density profiles. $\rho_n(z)$ represents the noise fluctuations which can be modeled as a Gaussian random process with certain standard deviation ($\sigma_{density}$). These fluctuations are damped with depth according to the damping factor α .

2.2. Grain Size

Assuming constant accumulation of snow with negligible densification the relationship between grain size of ice crystals and depth is written as:

$$r(z)^2 = r_{surface}^2 + Qz \quad (2)$$

where $r(z)$ is the grain size profile versus depth, $r_{surface}$ is the grain size at the surface, z is depth, and Q is the grain size gradient [10].

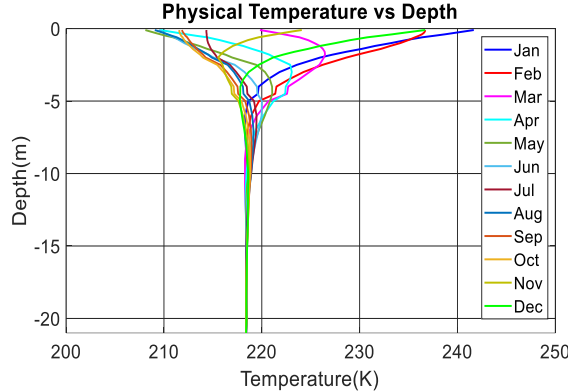


Figure 1: Monthly averaged in-situ firn temperature measurements versus depth at the Concordia station between 2006 and 2010 [11].

2.3. Firn Temperature

Monthly averaged physical temperature profiles measured at the Concordia station between 2006 and 2010 down to 21 meters depth [11], shown in Figure 1, are considered as ground truth firn temperature data. Below 21 meters, deep ice is considered isothermal with no temperature variations.

3. RADIATION MODEL

A simple microwave radiation model has been developed where the brightness temperatures at the firn surface for frequency f , incidence angle θ_i and polarization p , $T_B(z = 0, f, \theta_i, p)$, were analytically calculated using the following zeroth order radiative transfer equation:

$$T_B(z = 0, f, \theta_i, p) = \int_{z_{deep}}^{z=0} \left[\prod_{z'=z}^{z'=0} \Gamma(z', \theta(z'), p) \right] \kappa_e(f, z) \sec \theta(z) * T(z) e^{- \int_{z'=z}^{z'=0} \kappa_e(z', f) \sec \theta(z') dz'} dz \quad (3)$$

where $\Gamma(z', \theta(z'), p)$, $\theta(z')$ and $T(z)$ are the amplitude squared of the Fresnel transmission coefficient at the ice layer interface at depth z' for polarization p , the angle of incidence at the ice layer interface at depth z' , and the physical firn temperature at depth z , respectively. κ_e is the extinction coefficient which can be calculated using the formulas in [12].

4. GPM CONSTELLATION

The GPM mission is an international constellation-based mission which is designed to combine and improve precipitation measurements from several operational microwave sensors. Two GPM instruments, Special Sensor Microwave Imager/Sounder (SSMIS) and Advanced

Instrument	Frequency	Spatial Resolution	Polarization
AMSR2	6.9 GHz	62 x 35 km	V, H
AMSR2	7.3 GHz	62 x 35 km	V, H
AMSR2	10.65 GHz	42 x 24 km	V, H
AMSR2	18.7 GHz	22 x 14 km	V, H
SSMIS	19.35 GHz	72 x 44 km	V, H
SSMIS	22.235 GHz	72 x 44 km	V
AMSR2	23.8 GHz	26 x 15 km	V, H
AMSR2	36.5 GHz	12 x 7 km	V, H
SSMIS	37 GHz	44 x 26 km	V, H
AMSR2	89 GHz	5 x 3 km	V, H
SSMIS	91.655 GHz	15 x 9 km	V, H

Figure 2: SSMIS and AMSR2 frequency channels below 100 GHz with their polarization and spatial resolution information. Channels highlighted with red color are intercalibrated.

Microwave Scanning Radiometer-2 (AMSR2), owing to their polar orbits, have suitable measurements to study the polar firn. These sensors provide intercalibrated radiometric measurements over the Cryosphere at multiple frequencies below 100 GHz as shown in Figure 2 [13]. These intercalibrated multi-frequency measurements enable the use of the GPM constellation as a single radiometer to analyze polar ice sheets.

5. SIMULATIONS AND SATELLITE DATA

To validate the use of the radiation model described in section 3, to utilize the GPM constellation for polar studies, calculated brightness temperatures were compared to SSMIS and AMSR2 measurements over the Concordia Station in Antarctica.

For the simulations, density, grain size, and temperature of the polar firn were assumed to be as described in section 2. In the density model in equation (1), it was assumed that $\rho_\infty = 922 \text{ kg/m}^3$, $\rho_0 = 336 \text{ kg/m}^3$, $\beta = 0.017 \text{ m}^{-1}$, ρ_n is a Gaussian random process with zero mean and 120 kg/m^3 standard deviation, and $\alpha = 0.02 \text{ m}^{-1}$. The grain size model in equation (2) was used with $r_{surface} = 0.0016 \text{ m}$ and $Q = 4.72 \times 10^{-9} \text{ m}$. These values are consistent with previous in-situ measurements at the Concordia Station [11].

AMSR2 and SSMIS measurements for the entire year of 2018 were collected and averaged monthly over a $0.25^\circ \times 0.25^\circ$ degree latitude-longitude grids centered around the Concordia ($75^\circ 05' 59'' \text{S}$ $123^\circ 19' 56'' \text{E}$) station in Antarctica.

Figure 3 demonstrates the calculated and measured brightness temperatures versus month around the annual average for 10 SSMIS-AMSR2 frequencies (22.235 GHz channel of SSMIS is not included as this channel provides brightness temperatures only in one polarization). An overall match has been achieved at all frequencies. It can be seen that at low frequencies, e.g., 6.9 GHz, 7.3 GHz and 10.65GHz, the brightness temperatures do not vary significantly throughout the year as the penetration depth is large at these frequencies

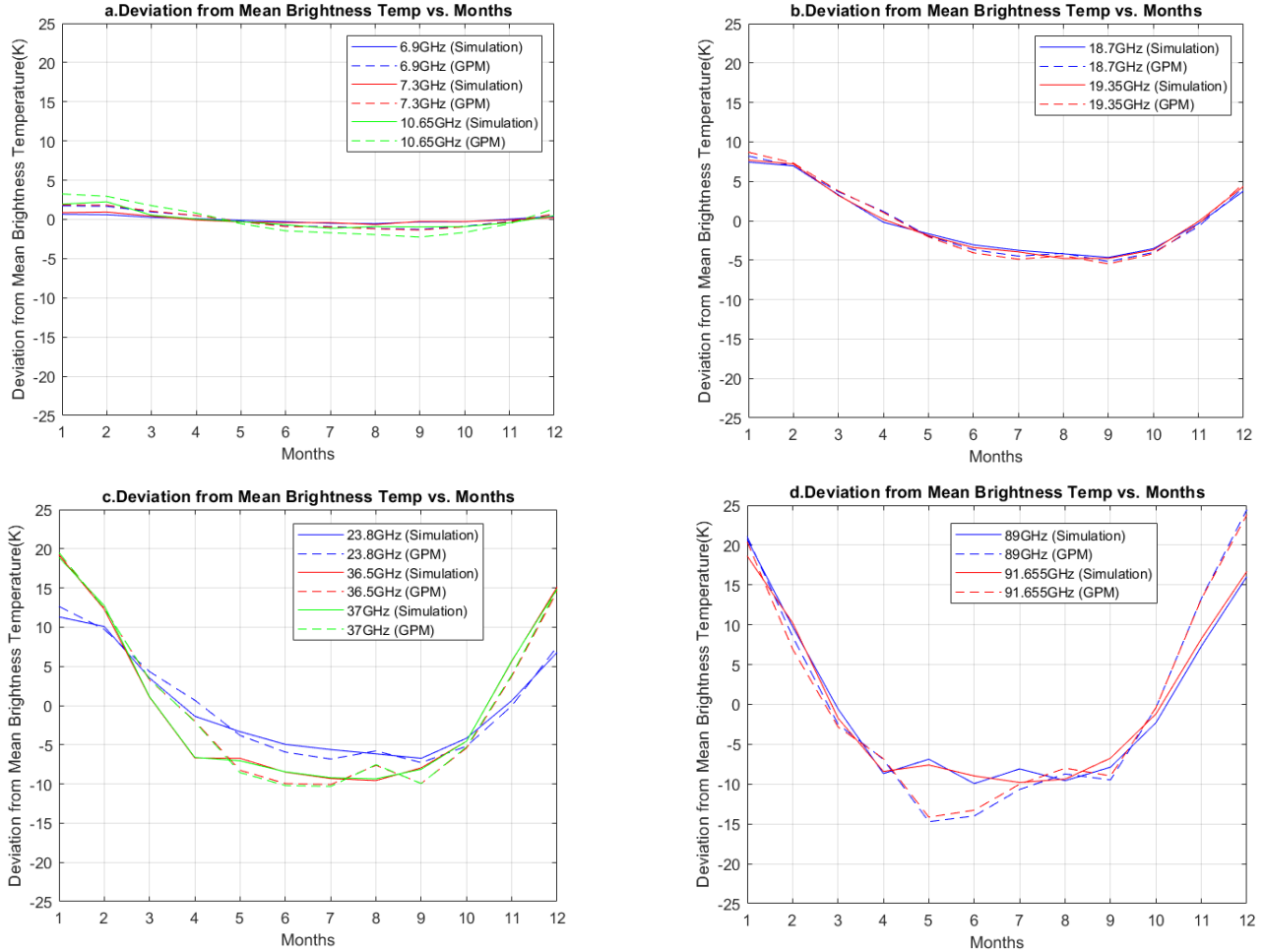


Figure 3: Measured Brightness Temperature over the Concordia station versus simulations at frequencies (a) 6.9 GHz, 7.3 GHz and 10.65 GHz; (b) 18.7 GHz and 19.35 GHz, (c) 23.8 GHz, 36.5 GHz, and 37 GHz; (d) 89 GHz and 91.65 GHz.

and the brightness temperatures reflect the temperatures of deep isothermal ice. On the other hand, at higher frequencies, e.g., 89 GHz and 91.65 GHz, the seasonal variations can be as large as 35 K as the brightness temperatures are mostly sensitive to the surface temperatures due to small electromagnetic penetration depths.

6. CONCLUSIONS

The results achieved in this study, i.e., highly correlated simulated brightness temperatures and satellite measurements shows the potential of the GPM constellation through its multi-frequency microwave radiometer measurements to characterize the polar firn. Figure 3 demonstrates that different frequencies are sensitive to the ice properties at different depths. Also, changing the parameters in ice models described in section 2 may result in significant changes in brightness temperatures as shown in Figure 4. In this figure, higher density fluctuations in the polar firn result

in lower brightness temperatures due to larger internal electromagnetic reflections. Thus, using simple regression techniques, such parameters can be estimated using the radiation models and satellite measurements. As future work, such numerical retrieval algorithms for the polar firn properties will be developed.

7. ACKNOWLEDGEMENT

This material is based on the work supported by the National Science Foundation under Grant no. 1844793.

The AMSR2 and SSMIS data were obtained from the NASA Goddard Space Flight Center's Precipitation Processing System (PPS) [14] and the Globe Portal System (G-Portal) of JAXA [15].

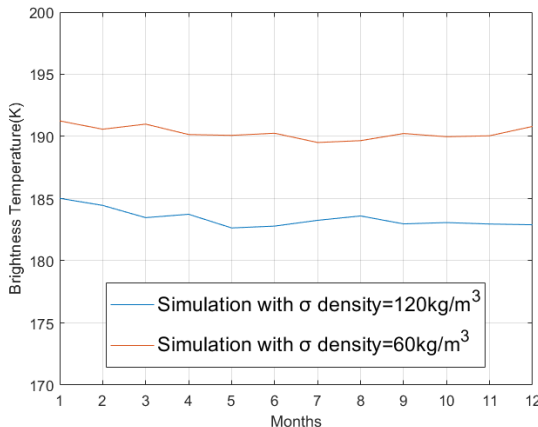


Figure 4: 6.9 GHz Brightness Temperature simulated with two different density fluctuation rates. Note the sensitivity of brightness temperatures to this parameter.

8. REFERENCES

[1] Aksoy, Mustafa, Joel T. Johnson, Kenneth C. Jezek, Michael Durand, Mark R. Drinkwater, Giovanni Macelloni, and Leung Tsang. "An examination of multi-frequency microwave radiometry for probing subsurface ice sheet temperature.", *In Proceedings of the 2014 IEEE Geoscience and Remote Sensing Symposium (IGARSS)*, Quebec City, Canada, 13-18 July 2014; pp. 3614-3617.

[2] Solomon, Susan, Martin Manning, Melinda Marquis, and Dahe Qin. *Climate change 2007—the physical science basis: Working group I contribution to the fourth assessment report of the IPCC*, Volume 4; Cambridge University Press: Cambridge, United Kingdom, 2007.

[3] Fujita, Shuji, Kumiko Goto-Azuma, Motohiro Hirabayashi, Akira Hori, Yoshinori Iizuka, Yuko Motizuki, Hideaki Motoyama, and Kazuya Takahashi. "Densification of layered firn in the ice sheet at Dome Fuji, Antarctica." *Journal of Glaciology* 62, no.231(2016): 103-123.

[4] Herron, Michael M and Chester C. Langway. "Firn densification: an empirical model." *Journal of Glaciology* 25, no.93(1980): 373-385.

[5] Zwally, H.Jay, Mario B. Giovinetto, Jun Li, Helen G. Cornejo, Matthew A. Beckley, Anita C. Brenner, Jack L. Saba, and Donghui Yi. "Mass changes of the Greenland and Antarctic ice sheets and shelves and contributions to sea-level rise: 1992–2002." *Journal of Glaciology* 51, no.175(2005): 509-527.

[6] Alley, Richard B, John F. Bolzan, and Ian M. Whillans. "Polar firn densification and grain growth." *Annals of Glaciology* 3(1982): 7-11.

[7] Nye, J.F. "Correction factor for accumulation measured by the thickness of the annual layers in an ice sheet." *Journal of Glaciology* 4, no. 36(1963):785-788.

[8] Aksoy, Mustafa. "Retrieval of Near-Surface Ice Sheet Properties Using the Global Precipitation Measurement (GPM) Radiometer Constellation." *2018 IEEE International Geoscience and Remote Sensing Symposium*, Valencia, 2018, pp. 5161-5164.

[9] Jezek, K.C, Joel T. Johnson, S.Tan, L.Tsang, Mark J. Andrews, M.Brogioni, G.Macelloni, M.Durand, C.C Chen, D.J Belgiovane, and Y.Duan. "500–2000-MHz brightness temperature spectra of the northwestern greenland ice sheet." *IEEE Transactions on Geoscience and Remote Sensing* 56, no.3(2017):1485-1496.

[10] Brucker, Ludovic, Ghislain Picard, and Michel Fily. "Snow grain-size profiles deduced from microwave snow emissivities in Antarctica." *Journal of Glaciology* 56, no.197(2010):514-526.

[11] Brucker, Ludovic, Ghislain Picard, Laurent Arnaud, Jean-Marc Barnola, Martin Schneebeli, Hélène Brunail, Eric Lefebvre, and Michel Fily. "Modeling time series of microwave brightness temperature at Dome C, Antarctica, using vertically resolved snow temperature and microstructure measurements." *Journal of Glaciology* 57, no.201(2011):171-182.

[12] Picard, Ghislain, Ludovic Brucker, Alexandre Roy, Florent Dupont, M.Fily, Alain Royer, and Chawn Harlow. "Simulation of the microwave emission of multi-layered snowpacks using the dense media radiative transfer theory: the DMRT-ML model." *Geosci. Model Dev. Discuss*, no.5(2012): 3647-3694

[13] Berg, Wesley, Stephen Bilanow, Ruiyao Chen, Saswati Datta, David Draper, Hamideh Ebrahimi, Spencer Farrar et al. "Intercalibration of the GPM microwave radiometer constellation." *Journal of Atmospheric and Oceanic Technology* 33, no. 12 (2016): 2639-2654.

[14] Precipitation Processing System. Available online: <https://pps.gsfc.nasa.gov/> (accessed on 1 June 2019).

[15] G-Portal, Globe Portal System. Available online: <https://gportal.jaxa.jp/gpr/?lang=en> (accessed on 1 June 2019).